TOXICOLOGICAL SCIENCES **77,** 172–182 (2004)
DOI: 10.1093/toxsci/kfh011

Modes of Cell Death in Rat Liver after Monocrotaline Exposure

Bryan L. Copple,* Catherine M. Rondelli,* Jane F. Maddox,* Niel C. Hoglen,† Patricia E. Ganey,* and Robert A. Roth*,[1]

Department of Pharmacology and Toxicology, Institute for Environmental Toxicology, and National Food Safety and Toxicology Center, Michigan State University, East Lansing, Michigan 48824 and †IDUN Pharmaceuticals, Inc., San Diego, California 92121

Received on July 24, 2003; accepted on October 1, 2003

Monocrotaline (MCT) is a pyrrolizidine alkaloid (PA) plant toxin that produces sinusoidal endothelial cell (SEC) injury, hemorrhage, fibrin deposition, and coagulative hepatic parenchymal cell (HPC) oncosis in centrilobular regions of rat livers. Cells with apoptotic morphology have been observed in the livers of animals exposed to other PAs. Whether apoptosis occurs in the livers of MCT-treated animals and whether it is required for full manifestation of pathological changes is not known. To determine this, rats were treated with 300 mg MCT/kg, and apoptosis was detected by transmission electron microscopy and the TUNEL (TdT-mediated dUTP nick end labeling) assay. MCT produced significant apoptosis in the liver by 4 h after treatment. To determine if MCT kills cultured HPCs by apoptosis, HPCs were isolated from the livers of rats and exposed to MCT. MCT caused a concentration-dependent release of alanine aminotransferase (ALT), a marker of HPC injury. Furthermore, caspase 3 was activated and TUNEL staining increased in MCT-treated HPCs. MCT-induced TUNEL staining and release of ALT into the medium were completely prevented by the pancaspase inhibitors z-VAD.fmk and IDN-7314, suggesting that MCT kills cultured HPCs by apoptosis. To determine if caspase inhibition prevents MCT-induced apoptosis in the liver, rats were cotreated with MCT and IDN-7314. IDN-7314 reduced MCT-induced TUNEL staining in the liver and release of ALT into the plasma. Morphometric analysis confirmed that IDN-7314 reduced HPC oncosis in the liver by approximately 50%. Inasmuch as HPC hypoxia occurred in the livers of MCT-treated animals, upregulation of the hypoxia-regulated cell-death factor, BNIP3 (Bcl2/adenovirus EIB 19kD-interacting protein 3), was examined. BNIP3 was increased in the livers of mice treated 24 h earlier with MCT. Results from these studies show that MCT kills cultured HPCs by apoptosis but causes both oncosis and apoptosis in the liver *in vivo*. Furthermore, caspase inhibition reduces both apoptosis and HPC oncosis in the liver after MCT exposure.

Key Words: **monocrotaline; liver; rat; apoptosis; caspase 3; BNIP3; hypoxia; oncosis.**

Monocrotaline (MCT) is a pyrrolizidine alkaloid (PA) plant toxin that produces liver injury in humans and animals (Huxtable, 1989; Schultze and Roth, 1998). People are exposed to PAs through consumption of herbal medicines made from PA-containing plants or by ingesting food grains contaminated with seeds or other components of PA-containing plants (Huxtable, 1989).

In the liver, MCT produces rapid sinusoidal and central venular endothelial cell injury, which results in severe hemorrhage, pooling of blood, and activation of the coagulation system (Copple *et al*., 2002a; Schoental and Head, 1955). The latter causes sinusoidal fibrin deposition in centrilobular regions (Copple *et al*., 2002a,b). These events precede the development of coagulative hepatic parenchymal cell (HPC) oncosis, which occurs at later times (Copple *et al*., 2002a). Apoptosis has been described in the livers of animals exposed to the PA, retrorsine (Gordon *et al*., 2000a,b), suggesting that PAs produce mixed lesions consisting of oncotic and apoptotic HPCs. Although HPC oncosis predominates in the livers of MCT-treated rats, studies have not determined if HPC apoptosis occurs as well.

Numerous hepatotoxicants produce apoptosis in liver. For example, HPC apoptosis is observed in the livers of animals exposed to acetaminophen (Gujral *et al*., 2002), ethanol (Yacoub *et al*., 1995), or galactosamine given with bacterial lipopolysaccharide (LPS) (Jaeschke *et al*., 1998). Lesions produced by these hepatotoxicants are mixed (i.e., contain regions of oncosis and apoptosis), and depending on the toxicant, apoptosis plays either a major or minor role in the overall pathogenesis. For example, inhibition of apoptosis in animals exposed to LPS and galactosamine with caspase inhibitors prevents the development of HPC oncosis, suggesting that apoptosis is causally involved in the development of later oncotic pathological changes (Jaeschke *et al*., 1998). By contrast, inhibition of apoptosis in animals exposed to acetaminophen has no effect on the development of the HPC oncosis, suggesting that apoptosis and oncosis occur independently (Lawson *et al*., 1999).

Based on these studies, it is clear that apoptosis and oncosis may occur independently or may be interdependent events. Given the observation that retrorsine causes both apoptosis and oncosis in liver, it was of interest to determine if MCT pro-

[1] To whom correspondence should be addressed at Department of Pharmacology and Toxicology, B-346 Life Sciences Building, Michigan State University, East Lansing, MI 48824. Fax: (517) 353-8915. E-mail: rothr@msu.edu.

duced HPC apoptosis in the liver and if apoptosis is required for full manifestation of pathological changes that occur in the livers of these animals. Accordingly, the studies presented here were designed to test the hypothesis that HPC apoptosis occurs in the liver after MCT exposure and contributes to oncotic liver injury.

MATERIALS AND METHODS

Animals. Male Sprague-Dawley rats (Crl:CD (SD)IGS BR, Charles River, Portage, MI) weighing 90–150 g and male C57BL/6 mice (Jackson Laboratories, Bar Harbor, ME) weighing 19–22 g were used for these studies. Rats weighing 90–150 g were used for these studies because MCT-induced liver injury was more consistent in this age group compared with older rats. Animals were allowed food (Rodent Chow/Tek 8640, Harlan Teklad, Madison, WI) and water *ad libitum*. Rats were housed no more than three to a cage, and mice no more than one to a cage on Aspen chip bedding (Northeastern Products Company, Warrenburg, NY). The animals were maintained on a 12-h light: dark cycle in a controlled temperature (18–21°C) and humidity (55 ± 5%) environment for a period of 1 week before use. All procedures on animals followed the guidelines for humane treatment set by the American Association of Laboratory Animal Sciences and the University Laboratory Animals Research Unit at Michigan State University.

Animal treatment protocol. MCT (Trans World Chemicals, Inc., Rockville, MD) was dissolved in sterile saline, minimally acidified by 2 M HCl. The pH was brought to 6.7 by addition of 4 M NaOH, and the volume was adjusted with sterile saline to the appropriate final concentration. Rats and mice were fasted for 24 h before treatment, because MCT-induced liver injury was more variable in fed animals. They received MCT or an equivalent volume of sterile saline vehicle by intraperitoneal (ip) injection between 3:00 and 5:00 P.M. Food was returned to the rats and mice immediately after MCT treatment. The injection volume for MCT was 2 ml/kg of rat or mouse.

To investigate the effect of IDN-7314 (IDUN Pharmaceuticals, San Diego, CA) on MCT-induced liver injury, rats were treated with 10 mg IDN-7314/kg or DMSO vehicle by ip injection and then with 300 mg MCT/kg or saline vehicle 30 min later. The injection volume for IDN-7314 solution and DMSO vehicle was 1 ml/kg of rat. Rats received additional administrations of 10 mg IDN-7314/kg or DMSO vehicle every 5 h thereafter for a total of four treatments. The rats were killed 18 h after MCT treatment.

To determine if hypoxia occurred in the livers of MCT-treated mice, mice were treated with 500 mg MCT/kg. This dose of MCT was used because 300 mg MCT/kg, used in the rat studies, did not produce liver injury in mice (data not shown). In addition, mice were used for some studies because BNIP3 (Bcl2/adenovirus EIB 19 kD-interacting protein 3) protein was measured in the liver using Western blot analysis, and the BNIP3 antibody did not cross-react with rat BNIP3. Mice then received 120 mg pimonidazole (Hypoxyprobe-1, NPI, Belmont, MA)/kg dissolved in sterile saline by ip injection 1 h before they were killed. Pimonidazole is rapidly reduced in hypoxic cells to a highly reactive intermediate that binds to sulfur on glutathione and proteins. An antibody has been raised against these pimonidazole-sulfur adducts, and immunohistochemistry is used to detect cells that contain them (i.e., hypoxic cells). This method has been used to detect hypoxic regions of liver (Arteel *et al*., 1995).

Pimonidazole immunohistochemistry. For pimonidazole immunostaining, paraffin-embedded sections were cut at 5 μm, deparaffinized, and stained for regions of hypoxia as described previously (Raleigh *et al*., 1998). Before immunostaining, sections were incubated with Biomeda pronase (Fisher Scientific, Pittsburgh, PA) for 40 min at 40°C. After three washes in phosphate-buffered saline (PBS) containing 0.2% Brij 35 (Sigma Chemical Co.), the sections were incubated with serum-free protein blocker (DAKO Corp. Carpinteria, CA) to block nonspecific staining. Next, the sections were incubated with pimonidazole monoclonal antibody (1:50) in PBS containing 0.2% Brij 35 and 1 drop of DAKO serum-free protein blocker/ml of antibody solution for 40 min at room temperature. They were then incubated for 3 h with goat anti-mouse secondary antibody conjugated to Alexa 594 (1:1000, Molecular Probes, Eugene, OR) in PBS containing 0.2% Brij 35 and 1 drop of DAKO serum-free protein blocker/ml of antibody solution. Sections were washed three times with PBS and visualized using a fluorescent microscope.

Assessment of hepatic injury, plasma fibrinogen and plasma hyaluronic acid. At various times after MCT treatment, the rats and mice were anesthetized with sodium pentobarbital (50 mg/kg, ip). A midline abdominal incision was made, and blood was collected from the descending aorta into a syringe containing sodium citrate (final concentration, 0.38%). HPC injury was evaluated by measuring the activity of alanine aminotransferase (ALT) in the plasma using Sigma Infinity ALT Kit (Sigma Chemical Co., St. Louis, MO).

One transverse section from the middle of the left lateral liver lobe and one from the right lateral lobe were fixed in 10% neutral buffered formalin for at least 3 days before being processed for histologic analysis. Additionally, a thin section (1.2 mm) of liver from the middle of the left lateral lobe was fixed in 4% glutaraldehyde in 0.1 M phosphate buffer for 24 h, processed, and analyzed by transmission electron microscopy (TEM) using a Philips 301 transmission electron microscope (FEI Company, Hillsboro, OR).

Paraffin-embedded sections were cut at 5 μm, stained with hematoxylin and eosin (H&E), and evaluated morphometrically for the size of the oncotic lesion as described in detail previously (Copple *et al*., 2002b).

Plasma fibrinogen concentration was determined from the thrombin clotting time of 200 μl of plasma diluted in imidazole buffer (provided in the kit) by using a fibrometer and a commercially available kit (Sigma Chemical Co. Kit 886-A). Plasma hyaluronic acid was measured using a commercially available, enzyme-linked immunosorbent assay (Chugai Diagnostics Science Co., Tokyo, Japan).

Ehrlich assay. The Ehrlich assay was used to measure the concentration of pyrroles in liver as a marker of bioactivation of MCT to toxic pyrrolic metabolites (Mattocks and White, 1970). This was done to determine whether IDN-7314 prevented bioactivation of MCT to MCT pyrrole (MCTP). The Ehrlich assay was performed as described in detail previously (Yee *et al*., 2000).

Isolation of HPCs from rats. HPCs were isolated from the livers of rats by collagenase perfusion as described in detail previously (Copple *et al*., 2003a). The viability of the HPCs was greater than 85%. The cells were resuspended in Williams' Medium E (Gibco, Grand Island, NY) supplemented with 10% fetal bovine serum (FBS; Intergen, Purchase, NY) and 1% gentamicin (Gibco) at a density of 2.5×10^5 cells/ml. The cells were cultured in Falcon 12-well plates (792 μl/well; BD Biosciences, Franklin Lakes, NJ) for viability studies or Falcon 4-well culture slides (1 ml/well) for TdT-mediated dUTP nick end labeling (TUNEL) staining. After a 2-h attachment period, the medium was removed and replaced with serum-free Williams' Medium E containing 1% gentamicin. The cells were then treated with MCT and/or caspase inhibitors.

Chemicals for cell culture studies. MCT was dissolved in serum-free Williams' medium E, minimally acidified by 2 M HCl. The pH was brought to 7.4 by addition of 4 M NaOH, and the volume was adjusted with serum-free Williams' medium E to a final concentration of 46 mM. IDN-7314 and *z*-VAD.fmk (Enzyme System Products, Livermore, CA) were reconstituted in DMSO to a final concentration of 20 mM. They were added to cultured HPCs at a final concentration of 20 μM. Therefore, the final volume of DMSO added to the medium was 1 μl/ml.

Assessment of cytotoxicity to cultured HPCs. HPCs were incubated with MCT and/or caspase inhibitors. After 18 h, the medium was collected, and the cells remaining on the plate were lysed with 1% Triton X-100 and sonication. Both the medium and the cell lysates were centrifuged at $600 \times g$ for 10 min. ALT activity in the cell-free supernatant fluids was determined by use of the Sigma Infinity ALT Kit (Sigma Chemical Co.). The ALT activity in the medium was expressed as a percentage of the total activity (i.e., activity in the medium plus activity in cell lysates). The percentage of ALT activity in the medium of untreated HPCs was then subtracted from the percentage of ALT

activity in the medium of all treatment groups. The resulting value was defined as the percent specific ALT release.

TUNEL assay. TUNEL staining was performed on sections of liver and cultured HPCs using a commercially available kit (*In Situ* Cell Death Detection Kit; Roche Diagnostics, Indianapolis, IN) as per manufacturer's recommendations. The HPCs were fixed in –20°C acetone for 10 min prior to staining.

Determination of caspase 3 activity. Caspase 3 activity was measured in HPC lysates using the Caspase 3 Assay Kit #2 (Molecular Probes, Eugene, OR) as per manufacturer's recommendations. Cleavage of a peptide substrate by caspase 3 to a fluorescent compound is the basis for this assay. Fluorescence was detected using a microplate spectrofluorometer (Spectra MAX Gemini; Molecular Devices Corp., Sunnyvale, CA), and the activity of caspase 3 was expressed as pmol/min/mg total protein. Protein concentrations of the samples were determined using the BCA assay (Pierce, Rockford, IL).

Western blot analysis. Cells were washed with PBS followed by lysis on ice with lysis buffer (0.01 M dibasic sodium phosphate, pH 7.2, 0.15 M sodium chloride, 10% Triton X-100, 12.7 mM deoxycholate, 1 mM sodium fluoride, 100 μg/ml phenylmethylsulphonyl fluoride, 100 μg/ml aprotinin, 1 mM sodium orthovanadate, 1 μg/ml pepstatin, and 1 μg/ml leupeptin). Protein concentrations of the samples were determined using the BCA assay. Aliquots (50 μg) of protein were subjected to 10% SDS–polyacrylamide gel electrophoresis, and separated proteins in the gel were transferred to Immobilon PVDF transfer membrane (Millipore, Bedford, MA). The blot was then probed with rabbit polyclonal antibody to NIP3 (BNIP3) followed by incubation with goat, anti-rabbit antibody conjugated to horseradish peroxidase (Santa Cruz Biotechnology, Santa Cruz, CA). The bands were detected using the ECL Western blotting detection kit (Amersham, Arlington Heights, IL).

Statistical analysis. Results are presented as the mean ± SEM. One-way or two-way multifactorial, completely random ANOVA was used to analyze treatment-related changes. ANOVAs were performed on log-transformed data in instances in which variances were not homogeneous. Data expressed as a percentage were transformed by arc sine square root prior to analysis. Comparisons among group means were made using the Student-Newman-Keuls test. The criterion for significance was $p < 0.05$ for all studies.

RESULTS

Apoptosis in the Liver After MCT Treatment.

Cells with apoptotic morphology (i.e., plasma membrane blebbing, shrunken cytoplasm, and condensed and marginated nuclear chromatin) were detected by TEM in sections of livers from rats treated 18 h earlier with MCT (Fig. 1A). These results were confirmed by light microscopic evaluation for detection of TUNEL-positive cells. Because oncotic cells can occasionally stain using this method (Gujral *et al*., 2002), only cells with nuclear TUNEL staining having morphologic characteristics of apoptosis (described above) were considered apoptotic. At early times after MCT exposure (i.e., 4 and 8 h), the distribution of apoptotic cells was panlobular, although more occurred in centrilobular regions (Fig. 1B). At later times when HPC oncosis was present (i.e., 12 and 18 h after MCT administration), apoptotic cells in centrilobular regions appeared only at the periphery of the oncotic foci. The number of TUNEL-positive cells was significantly increased in the liver by 4 h after MCT exposure and increased further at times thereafter (Fig. 1C).

MCT Cytotoxicity in Rat HPCs in Vitro

MCT was toxic to HPCs in a concentration-dependent manner as measured by release of ALT into the medium 18 h after treatment (Fig. 2). Significant ALT release occurred from HPCs treated 8 h earlier with 1.6 mM MCT (data not shown). By contrast, no ALT was released from HPCs treated 8 h earlier with the smaller concentrations of MCT tested (data not shown). To determine if signal transduction pathways that cause apoptosis were activated in MCT-treated HPCs, caspase 3 activity was determined. HPCs treated with TNF-α and actinomycin D were used as a positive control, and caspase 3 activity increased in these cells by 8 h, then decreased to baseline level by 18 h (Fig. 3A). Significant caspase 3 activity was not detected in HPCs treated with 0.01 mM MCT (Fig. 3B). At larger concentrations, MCT caused a concentration- and time-dependent increase in caspase 3 activity (Fig. 3B).

MCT-induced apoptosis was confirmed using the TUNEL assay. Approximately 13% of HPCs treated 18 h earlier with vehicle were TUNEL-positive (Figs. 4A and 4C). MCT caused a concentration-dependent increase in the percentage of TUNEL-positive cells (Figs. 4B and 4C).

Inhibition of MCT-Induced HPC Toxicity in Cell Culture with Caspase Inhibitors

To examine the effect of caspase inhibitors on MCT-induced damage in culture, HPCs were cotreated with MCT and the pancaspase inhibitors z-VAD.fmk or IDN-7314. Treatment of primary rat HPCs with 0.2 or 0.4 mM MCT produced a significant increase in the percentage of TUNEL-positive cells and in HPC toxicity as measured by release of ALT into the medium (Fig. 5). These increases were completely prevented by *z*-VAD.fmk or by IDN-7314 pretreatment.

Effect of IDN-7314 on MCT-Induced Liver Injury

To investigate the effect of caspase inhibition on MCT-induced liver injury *in vivo*, rats were cotreated with MCT and IDN-7314. By 18 h after treatment, MCT produced a significant increase in the number of TUNEL positive cells (Fig. 6A) and HPC injury, as measured by release of ALT into the plasma (Fig. 6B). IDN-7314 reduced the increase in TUNEL-positive cells by ~75% (Fig. 6A) and the increase in plasma ALT activity by ~65% (Fig. 6B).

Histopathological evaluation of livers from rats treated 18 h earlier with MCT and DMSO vehicle showed central venular endothelial cell (CVEC) injury, severe sinusoidal hemorrhage, and regions of coagulative HPC oncosis (i.e., swollen, eosinophilic cytoplasm; indistinct cell borders; pyknotic or karyolytic nuclei) in centrilobular regions (Fig. 7A). In addition, cells with apoptotic morphology were observed with a panlobular distribution (Fig. 7A). In rats cotreated with MCT and IDN-7314, the extent of CVEC injury and sinusoidal hemorrhage was similar to that observed in livers of rats treated with MCT

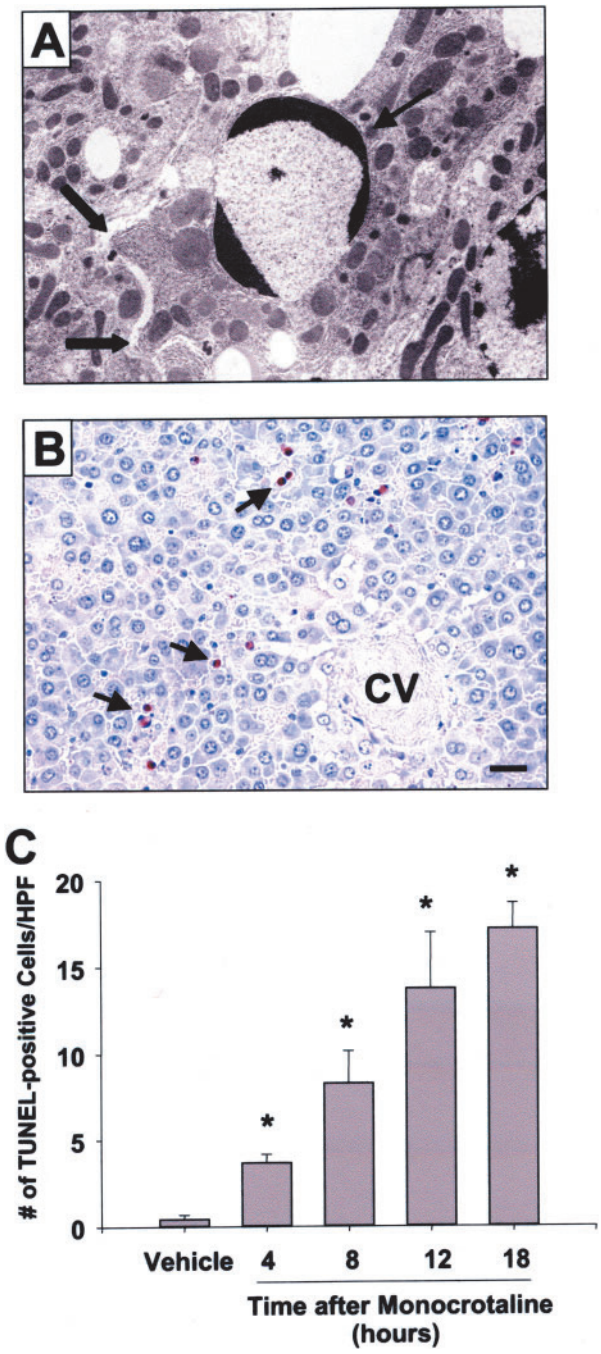

FIG. 1. Apoptosis in the liver after MCT treatment. (A) TEM photomicrograph (magnification ×7100) of a liver section from a rat treated 18 h earlier with MCT showing an apoptotic HPC. Broad arrows indicate regions of plasma membrane blebbing. Line arrow indicates a region of condensed and marginated nuclear chromatin. (B) Representative photomicrograph showing TUNEL staining of a liver section from a rat treated 8 h earlier with MCT. Arrows indicate TUNEL-positive cells (i.e., brown nuclear staining). CV = central vein. Bar represents 25 μm. (C) TUNEL-positive cells with apoptotic morphology (i.e., shrunken cytoplasm and condensed and marginated nuclear chromatin) in 20 random ×400 fields were counted in sections of stained livers. There were approximately 340 HPCs/high-powered field. Liver sections from saline-treated rats evaluated at different times were combined into 1 group, since no differences were observed among them. Data are expressed as means ± SEM; $n = 3$ rats/group. *Significantly different ($p < 0.05$) from vehicle-treated rats.

and vehicle (Fig. 7B). By contrast, the level of HPC oncosis and apoptosis was dramatically decreased (Fig. 7B).

Morphometric analysis of livers from rats treated with MCT and DMSO vehicle revealed that approximately 43% of the liver contained lesions consisting of oncotic HPCs (Fig. 7C). By contrast, only 19% of the liver area contained oncotic lesions after treatment with MCT and IDN-7314 (Fig. 7C).

Effect of IDN-7314 on MCT Bioactivation

Since MCT hepatotoxicity requires cytochrome P450-mediated bioactivation of MCT to a reactive pyrrolic metabolite (MCTP), it seemed possible that IDN-7314 exerted its protective effect by inhibiting MCT metabolism. To explore this possibility, rats were treated with IDN-7314 and MCT as described above, and tissue pyrrole concentration was determined in the liver 1.5 h after MCT administration. At this time, the bioactivation of MCT to MCTP is nearly complete (Allen *et al.*, 1972). The concentration of pyrrole in the liver after treatment with MCT and DMSO vehicle was 28.8 ± 2.7 μg/g of liver tissue, and after treatment with MCT and IDN-7314 the concentration was 33.4 ± 3.6 μg/g of liver tissue. These values were not statistically different, suggesting that IDN-7314 had no significant effect on MCT bioactivation.

Effect of IDN-7314 on MCT-Induced SEC Injury and Activation of the Coagulation System

To determine whether IDN-7314 prevented MCT-induced damage to sinusoidal endothelial cells (SECs) in the liver, plasma hyaluronic acid was measured as a marker of injury to these cells. Treatment of rats with MCT produced a significant increase in the plasma concentration of hyaluronic acid

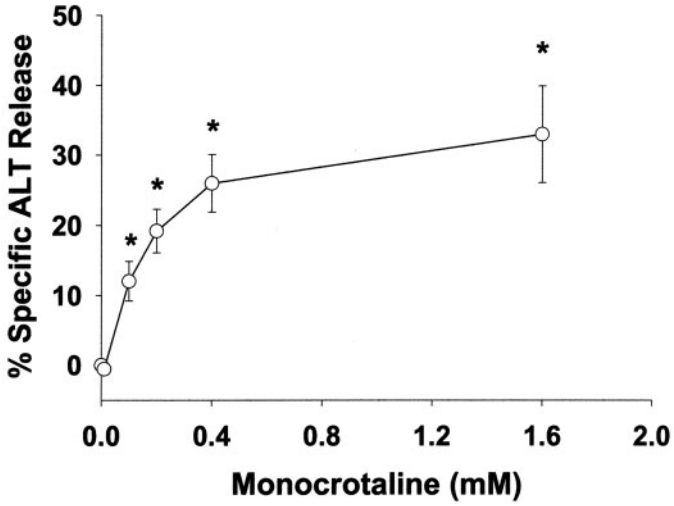

FIG. 2. MCT-induced cytotoxicity in primary rat HPCs. HPCs were exposed to 0.01, 0.1, 0.2, 0.4, or 1.6 mM MCT. Cytotoxicity was determined by release of ALT into the medium after 18 h of incubation. Data are expressed as means ± SEM; $n = 3$ (each n represents HPCs isolated from a different rat). *Significantly different ($p < 0.05$) from vehicle-treated HPCs.

(Fig. 8A), indicating impaired SEC function. This increase was not affected by IDN-7314 treatment (Fig. 8A).

Previous studies showed that the coagulation system is activated in MCT-treated rats, leading to a decrease in fibrinogen, and that this activation is required for HPC oncosis (Copple *et al*., 2002a,b). In the present studies, treatment with MCT and DMSO vehicle caused a significant decrease in plasma fibrinogen by 18 h that was unaffected by treatment with IDN-7314 (Fig. 8B).

Upregulation of BNIP3 in the Livers of MCT-Treated Mice

The observation of fibrin deposition (Copple *et al*., 2002a) and hemorrhage (Fig. 7) in livers of MCT-treated rats suggests the possibility of disrupted blood flow and centrilobular hypoxia. BNIP3 (Bcl2/adenovirus EIB 19 kD-interacting protein 3) is a proapoptotic protein upregulated in hypoxic cells. It is expressed as a 60 kD dimer in several cell types (Sowter *et al*., 2001). To determine if BNIP3 was upregulated in the livers of MCT-treated animals, mice were treated with MCT, and BNIP3 was detected in the liver. Mice were used for these studies because an anti-rat BNIP3 antibody was not available. To confirm that the pathological changes that occur in the livers of MCT-treated mice are similar to those in rats, mice were treated with 500 mg MCT/kg, and SEC injury and HPC injury were measured. Treatment of mice with MCT produced a significant increase in plasma concentration of hyaluronic acid by 8 h after treatment (Table 1). This was followed by a significant increase in plasma activity of ALT by 12 h after treatment (Table 1). Next it was determined if hypoxia occurs

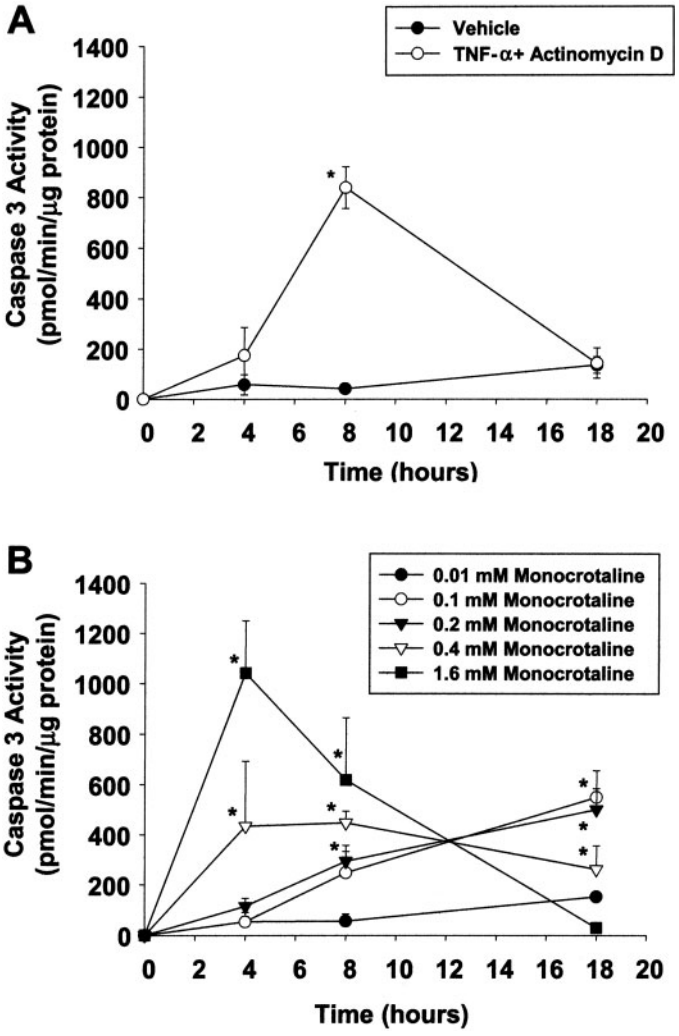

FIG. 3. Activation of caspase 3 in MCT-treated HPCs. Isolated HPCs were exposed to (A) TNF-α (2,000 U/ml) and actinomycin D (0.2 μg/ml) or (B) the indicated concentrations of MCT. Caspase 3 activity was measured in cell lysates at various times thereafter. Data are expressed as means ± SEM; $n = 3$ (each n represents HPCs isolated from a different rat). *Significantly different ($p < 0.05$) from vehicle-treated HPCs at the same time.

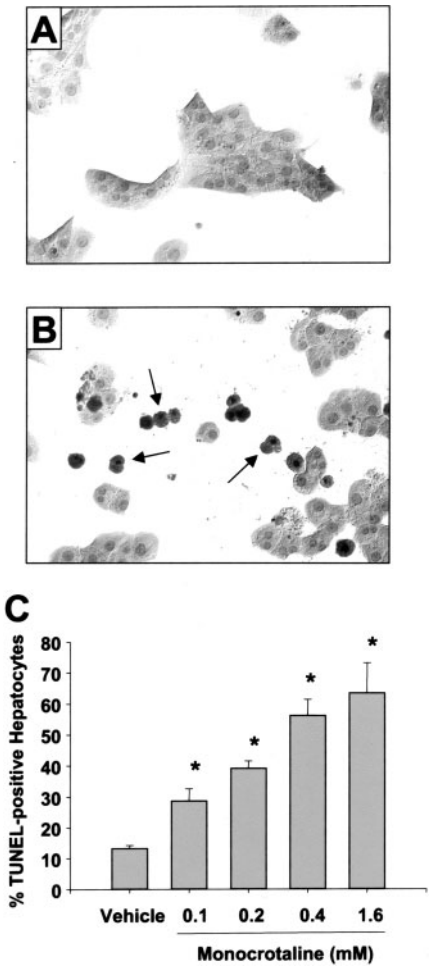

FIG. 4. TUNEL staining of HPCs treated with MCT. Representative photomicrographs are shown of HPCs treated with (A) vehicle or (B) 0.2 mM MCT 18 h earlier and stained using the TUNEL assay. (C) TUNEL-positive cells with apoptotic morphology (i.e., shrunken cytoplasm and condensed nuclear chromatin) in 10 random ×400 fields were counted in cultures of HPCs. Data are expressed as means ± SEM; $n = 3$ (each n represents HPCs isolated from a different rat). *Significantly different ($p < 0.05$) from vehicle-treated HPCs.

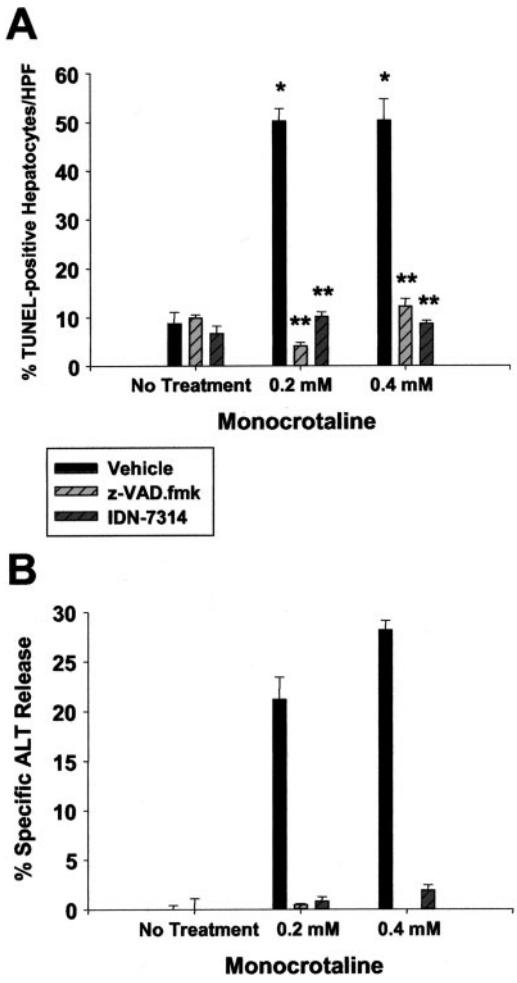

FIG. 5. Effect of caspase inhibitors on MCT-induced killing of HPCs. HPCs were exposed to 0.2 or 0.4 mM MCT in the presence or absence of 20 μM z-VAD.fmk, 20 μM IDN-7314, or DMSO vehicle. (A) The cultures were stained for apoptosis using the TUNEL assay 18 h after MCT exposure. TUNEL-positive cells with apoptotic morphology in 10 random ×400 fields were counted. (B) Cytotoxicity was determined by release of ALT into the medium after 18 h of incubation. Data are expressed as means ± SEM. $n = 3$ (each n represents HPCs isolated from a different rat). *Significantly different ($p < 0.05$) from HPCs that did not receive MCT. **Significantly different ($p < 0.05$) from HPCs treated with MCT and vehicle.

in the livers of MCT-treated mice. Hypoxia was detected in the livers of mice using immunohistochemical staining to detect pimonidazole-sulfur adducts, which are only present in hypoxic cells. Positive immunostaining for hypoxia was observed in centrilobular regions of the livers of mice treated 12 and 24 h earlier with MCT (Fig. 9). These studies confirmed that SEC injury and HPC injury occur with a similar time-course and sequence in mice and rats. Furthermore, these studies showed that hypoxia occurred in the livers of MCT-treated mice. Low levels of BNIP3 were detected by Western blot analysis as a 60 kD signal in livers from vehicle-treated mice (Fig. 10A). The level of BNIP3 was increased in the livers of mice treated 24 h earlier with MCT (Fig. 10A). Densitometry confirmed these results and showed that BNIP3 was significantly elevated in the livers of MCT-treated mice (Fig. 10B).

DISCUSSION

Apoptosis has been observed in livers of animals exposed to the PAs, riddelliine or retrorsine, and in a human patient who consumed an herbal concoction containing PAs (Gordon *et al*., 2000a,b; Nyska *et al*., 2002; Steenkamp *et al*., 2001). In results presented here, a time-dependent increase in the number of cells with apoptotic morphology was detected in livers of rats exposed to MCT. Based upon their size and location within the hepatic cords, many of these cells were HPCs. Occasionally,

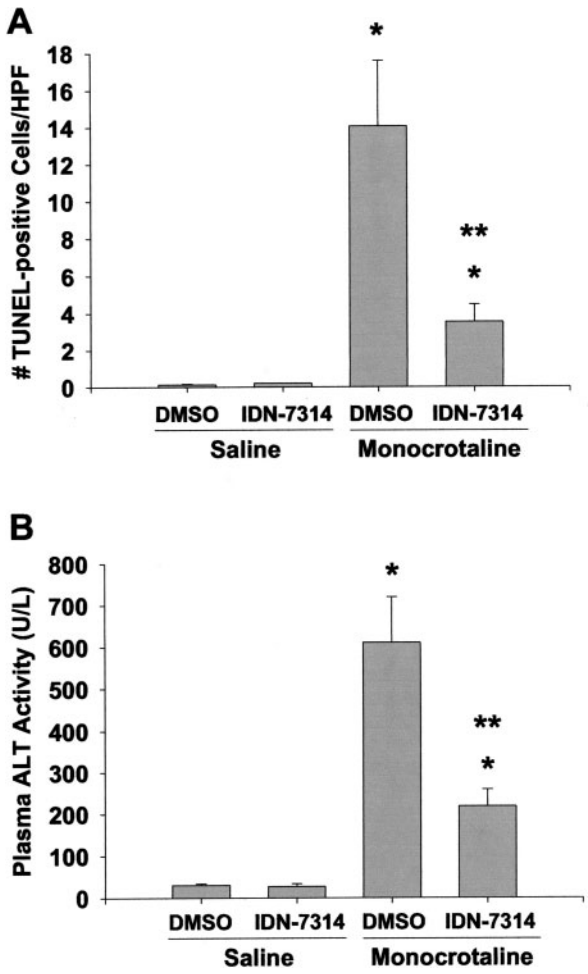

FIG. 6. Effect of IDN-7314 on MCT-induced liver injury. Rats were treated with IDN-7314 and MCT as described in the Materials and Methods. Livers were removed and plasma collected 18 h after MCT treatment. (A) The TUNEL assay and morphological criteria were used to detect apoptotic cells, which were counted in 20 random ×400 fields. (B) The activity of ALT was measured in the plasma. Data are expressed as means ± SEM. $n = 3$ for rats treated with DMSO/saline or IDN-7314/saline; $n = 8$ for rats treated with DMSO/MCT or IDN-7314/MCT *Significantly different ($p < 0.05$) from corresponding saline-treated control. **Significantly different ($p < 0.05$) from rats treated with MCT and DMSO.

however, small apoptotic cells were detected within the sinusoids, and it is possible that these cells were apoptotic SECs. Apoptotic endothelial cells have been observed in the livers of rats exposed to riddelliine (Nyska *et al*., 2002). Furthermore, MCTP, the toxic metabolite of MCT, induces apoptosis in cultured pulmonary artery endothelial cells (Thomas *et al*., 1998).

HPC oncosis occurred primarily in centrilobular regions of MCT-treated rats, whereas apoptosis occurred with a panlobular distribution outside of the regions of oncosis. The reason for this difference in distribution is unknown, but it may be related to the degree of MCT metabolite formation. MCT must be metabolized by cytochromes P450 to become toxic (Lafranconi and Huxtable, 1984; Pan *et al*., 1993). The P450s responsible for this metabolism are primarily located in centrilobular regions (Oinonen and Lindros, 1998). Therefore, HPCs in centrilobular regions would be exposed to greater concentrations of toxic MCT metabolites. Studies *in vitro* have shown that PAs kill cultured human hepatoma cells by apoptosis at small concentrations and oncosis at larger concentrations (Steenkamp *et al*., 2001). Therefore, HPCs in centrilobular regions exposed to large concentrations of toxic MCT metabolite might be expected to die by oncosis, whereas cells in other regions of the liver exposed to smaller concentrations may die by apoptosis.

In addition to causing apoptosis *in vivo*, MCT caused concentration-dependent increases in caspase 3 activity and in

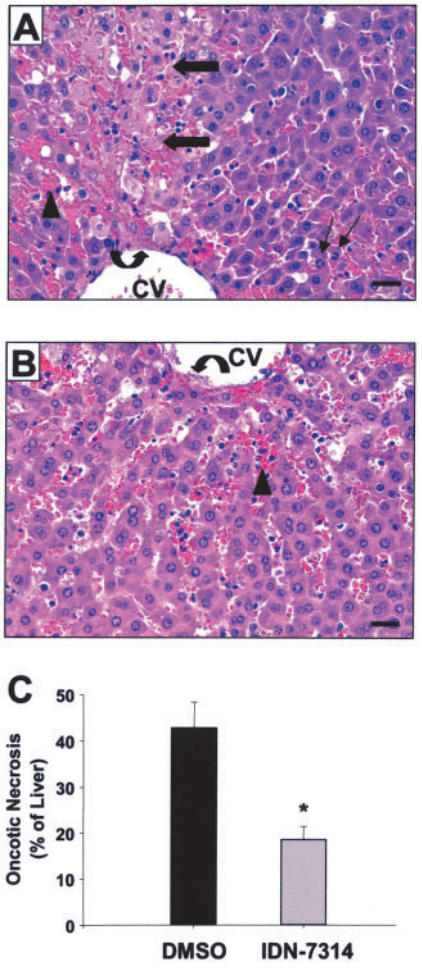

FIG. 7. Effect of IDN-7314 on MCT-induced oncosis in the liver. Rats were treated with IDN-7314 and MCT as described in Materials and Methods. Livers were removed 18 h after MCT treatment and stained with H&E. (A) Liver from a rat treated with MCT and saline. (B) Liver from a rat treated with MCT and IDN-7314. Broad arrows indicate coagulative oncosis. Curved arrows indicate CVEC injury. Arrowheads indicate hemorrhage. Line arrows indicate apoptotic HPCs. Bar represents 25 μm. (C) The area of HPC oncosis was quantified as described previously (Copple *et al*., 2002b). Data are expressed as means ± SEM. $n = 8$ rats per group. *Significantly different ($p < 0.05$) from rats treated with MCT and DMSO.

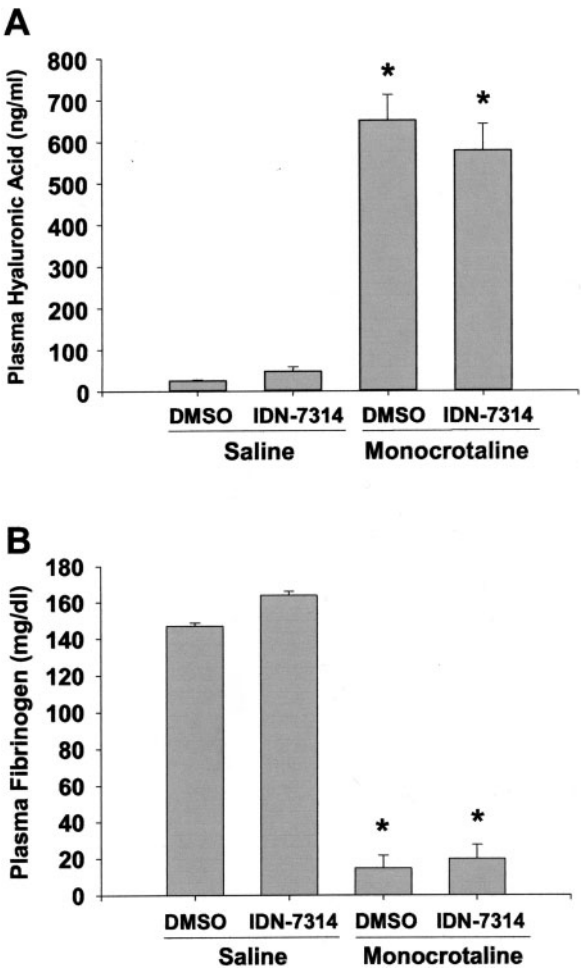

FIG. 8. Effect of IDN-7314 on MCT-induced SEC injury and activation of the coagulation system. Rats were treated with IDN-7314 and MCT as described in Materials and Methods. Plasma was collected 18 h after MCT treatment. (A) Plasma hyaluronic acid was evaluated as a marker of SEC injury. (B) Plasma fibrinogen was evaluated as a marker of activation of the coagulation system. Data are expressed as means ± SEM. $n = 3$ for rats treated with DMSO/saline or IDN-7314/saline; $n = 8$ for rats treated with DMSO/MCT or IDN-7314/MCT *Significantly different ($p < 0.05$) from corresponding saline-treated control.

TABLE 1
Sinusoidal Endothelial Cell and Hepatic Parenchymal Cell Injury in Livers of MCT-Treated Mice.

		Time after MCT		
Biomarker	Vehicle	8 h	12 h	24 h
Hyaluronic acid (ng/ml)	416 ± 67	1447 ± 178[a]	1280 ± 224[a]	1190 ± 246[a]
ALT (U/L)	48 ± 14	64 ± 9	132 ± 34[a]	4012 ± 1353[a]

Note. Mice were treated with saline vehicle or 500 mg MCT/kg (ip). Plasma hyaluronic acid concentration and ALT activity were evaluated 8, 12, and 24 h after treatment. Data are expressed as means ± SEM. $n = 4–6$ mice/group.
[a]Significantly different ($p < 0.05$) from saline-treated control.

numbers of apoptotic HPCs *in vitro*. The pancaspase inhibitors z-VAD.fmk and IDN-7314 completely prevented the increased number of apoptotic cells and the release of ALT into the medium (Fig. 5). These results suggest that MCT kills HPCs exclusively by apoptosis *in vitro*. This is in contrast to what occurs *in vivo*. In rats treated 18 h earlier with MCT, a majority of dead HPCs had oncotic morphology, whereas few died by apoptosis. The reason for the discrepancy between observations *in vitro* and *in vivo* is not known, but the results suggest that HPC oncosis *in vivo* occurs not only from direct MCT toxicity but involves a contribution also by indirect mechanisms that are not reproduced *in vitro*. For example, the coagulation system is activated after MCT exposure, causing sinusoidal fibrin deposition (Copple *et al*., 2002a). Furthermore, anticoagulants prevent HPC oncosis, suggesting that the coagulation system is causally involved in HPC oncosis (Copple *et al*., 2002b). Although it is unclear how the coagulation system contributes to MCT hepatotoxicity, the mechanism by which it promotes HPC injury would not be reproduced in cultures of MCT-treated HPCs.

IDN-7314 decreased apoptosis in the livers of MCT-treated rats by approximately 75% (Fig. 6A) and reduced the increase in plasma ALT to a similar extent (Fig. 6B). An increase in ALT in the plasma is typically considered an indicator of HPC oncosis, since HPCs must lose plasma membrane integrity for ALT to be released. Therefore, these results suggested that IDN-7314 not only reduced MCT-induced apoptosis but also reduced HPC oncosis. This suggestion was corroborated by morphometric analysis, which revealed approximated 60% reduction in oncotic area (Fig. 7C).

How IDN-7314 reduced MCT-induced HPC oncosis is not known, but its effect is not due to altered MCT bioactivation, since similar levels of MCTP were formed in the livers of rats treated with MCT and DMSO or MCT and IDN-7314. Furthermore, IDN-7314 had no effect on MCT-induced SEC injury (Fig. 8A) or on activation of the coagulation system (Fig. 8B), two early events thought to be causally involved in MCT-induced HPC injury (Copple *et al*., 2002a,b). Thus, caspases likely come into play after these early events to participate in MCT hepatotoxicity.

Reduction of toxicant-induced HPC oncosis by caspase inhibitors has been described previously. For example, cotreatment of rats with bacterial lipopolysaccharide plus galactosamine produces a mixed liver lesion consisting of both apoptotic and oncotic HPCs (Jaeschke *et al*., 2000). In this model, caspase inhibition prevents both HPC apoptosis and oncosis (Jaeschke *et al*., 2000). This occurs because HPC apoptosis stimulates transmigration of neutrophils (PMNs) from the sinusoids into the parenchyma (Lawson *et al*., 1998), and these inflammatory cells cause HPC oncosis at later times. It is unlikely that this occurs after MCT treatment, since PMNs and other inflammatory mediators are not required for MCT-induced HPC oncosis (Copple *et al*., 2003b).

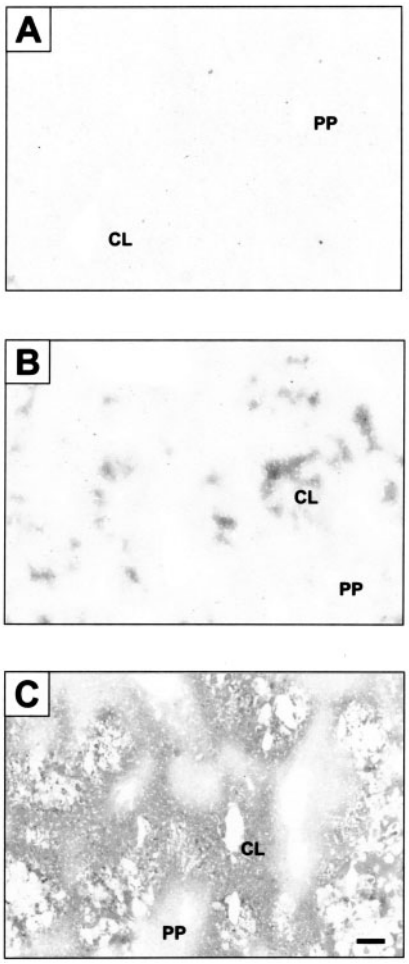

FIG. 9. Hypoxia in the livers of MCT-treated mice. Mice were treated with saline vehicle or 500 mg MCT/kg (ip). They received 120 mg pimonidazole/kg by ip injection 1 h before they were killed. Livers were removed 12 or 24 h after treatment and processed for immunohistochemical staining of hypoxia, which appears gray in the photomicrographs. Depicted are liver sections from a mouse treated 24 h earlier with saline (A) and from mice treated (B) 12 or (C) 24 h earlier with MCT. CL, centrilobular; PP, periportal. Bar represents 100 μm.

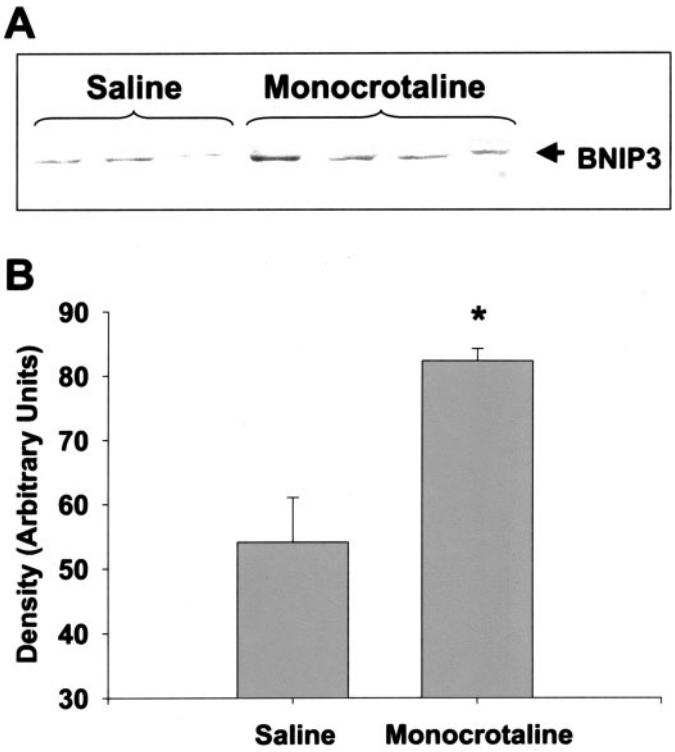

FIG. 10. Upregulation of BNIP3 in the livers of MCT-treated mice. Mice were treated with saline vehicle or 500 mg MCT/kg (ip). Livers were removed 24 h later, and the level of BNIP3 was assessed by Western blot analysis. (A) Representative BNIP3 Western blot. (B) The densities of the BNIP3 bands were quantified using a densitometer. Data are expressed as means ± SEM. $n = 3$ for saline-treated mice; $n = 4$ for MCT-treated mice. *Significantly different ($p < 0.05$) from corresponding saline-treated control.

A second possibility is that hypoxia-induced depletion of hepatocellular ATP switches MCT-induced cell death from apoptosis to oncosis. Apoptosis is an ATP-dependent process (Eguchi *et al*., 1997; Leist *et al*., 1997), and agents that produce apoptosis under normal conditions produce oncosis when cellular ATP is depleted (Leist *et al*., 1997). For example, activation of the CD95 receptor in T cells produces apoptosis; reduction of cellular ATP levels with oligomycin prior to CD95 activation, however, causes these cells to die by oncosis (Leist *et al*., 1997). Furthermore, z-VAD.fmk prevented both types of cell death induced by CD95, suggesting that they shared similar signal transduction pathways at early stages. A similar phenomenon might occur in the livers of MCT-treated animals. Hypoxia occurs in centrilobular regions of livers of MCT-treated mice where HPC oncosis develops (Fig. 9). Recent studies have shown that prolonged periods of hypoxia in the liver can reduce cellular ATP levels (Paxian *et al*., 2003). Therefore, HPCs in the liver that are exposed to sufficient concentrations of MCT may begin to die by apoptosis, however, HPCs in hypoxic regions may experience ATP depletion, thereby switching the mode of cell death to oncosis. Caspase inhibitors would be expected to prevent this injury since the initial mechanism by which these cells began to die occurred through caspase-dependent pathways. By contrast, HPCs outside of the regions of hypoxia would die by apoptosis. This is consistent with histopathological changes that occur in the livers of MCT-treated animals. Apoptotic HPCs were distributed panlobularly at early times when hypoxia was absent. At later times, however, apoptotic cells were only detected outside of the regions of hypoxia, and dead HPCs in hypoxic centrilobular regions were oncotic. Further studies will need to be conducted to determine if this mechanism contributes to HPC oncosis in MCT-treated animals.

Finally, it is possible that oncotic HPCs in centrilobular regions die from exposure to extreme hypoxia. Prolonged periods of hypoxia in the liver produce HPC injury (Lemasters *et al*., 1981; Paxian *et al*., 2003; Thurman *et al*., 1984). Since hypoxia occurs in the livers of MCT-treated mice (Fig. 9), it might be causally involved in HPC toxicity. Hypoxia activates signal transduction pathways that can lead to death of cells. For example, it stabilizes hypoxia-inducible factor-1α (HIF-1α), a transcription factor, which translocates to the nucleus and heterodimerizes with HIF-1β (also called ARNT, arylhydrocarbon nuclear translocator) (Semenza, 1999). These proteins interact with transcriptional coactivators to upregulate expression of numerous genes, including some involved in cell death. One of these, BNIP3, is a proapoptotic member of the Bcl-2 family of proteins that promotes death of cells through diverse pathways depending on the cell type (Kubasiak *et al*., 2002; Lamy *et al*., 2003; Regula *et al*., 2002; Vande Velde *et al*., 2000). Death initiated by this protein occurs through caspase-dependent (Regula *et al*., 2002) or -independent mechanisms (Kubasiak *et al*., 2002; Vande Velde *et al*., 2000). Furthermore, cells that die by BNIP3-mediated pathways can exhibit morphological characteristics of either oncosis (Vande Velde *et al*., 2000) or apoptosis (Lamy *et al*., 2003). In the livers of MCT-treated animals, it is possible that HPCs exposed to extremely hypoxic conditions in centrilobular regions die by a BNIP3-related mechanism. In support of this hypothesis, increased expression of BNIP3 was observed in livers of MCT-treated mice (Fig. 9). Unfortunately, the antibody used for these studies could not detect BNIP3 using immunohistochemistry; therefore, it was not possible to show that HPCs specifically in hypoxic centrilobular regions expressed this protein. Although these results suggest that BNIP3 could contribute to MCT-induced liver injury, additional studies are clearly needed to address this hypothesis fully.

In summary, apoptosis occurred in the livers of MCT-treated rats. Furthermore, caspase inhibition prevented the development of both HPC oncosis and apoptosis. Activation of caspase 3, increased TUNEL staining, and release of ALT were observed in primary rat HPCs treated with MCT. Caspase inhibition completely prevented TUNEL staining and release of ALT from these cells, suggesting that they die by apoptosis.

Cotreatment of rats with MCT and a pancaspase inhibitor prevented both HPC oncosis and apoptosis. Finally, the hypoxia-regulated cell-death factor, BNIP3, was upregulated in liver after MCT exposure, suggesting that hepatocellular hypoxia increases this factor, leading to caspase activation and HPC oncosis.

ACKNOWLEDGMENTS

This study was supported by NIH Grants ES04139 and DK50728. B.L.C. was supported in part by NRSA ES05866 from NIH. We thank Dr. Gavin Arteel for advice on pimonidazole staining.

REFERENCES

Allen, J. R., Chesney, C. F., and Frazee, W. J. (1972). Modifications of pyrrolizidine alkaloid intoxication resulting from altered hepatic microsomal enzymes. *Toxicol. Appl. Pharmacol*. **23,** 470–479.

Arteel, G. E., Thurman, R. G., Yates, J. M., and Raleigh, J. A. (1995). Evidence that hypoxia markers detect oxygen gradients in liver: Pimonidazole and retrograde perfusion of rat liver. *Br. J. Cancer* **72,** 889–895.

Copple, B. L., Banes, A., Ganey, P. E., and Roth, R. A. (2002a). Endothelial cell injury and fibrin deposition in rat liver after monocrotaline exposure. *Toxicol. Sci.* **65,** 309–318.

Copple, B. L., Woolley, B., Banes, A., Ganey, P. E., and Roth, R. A. (2002b). Anticoagulants prevent monocrotaline-induced hepatic parenchymal cell injury but not endothelial cell injury in the rat. *Toxicol. Appl. Pharmacol*. **180,** 186–196.

Copple, B. L., Moulin, F., Hanumegowda, U. M., Ganey, P. E., and Roth, R. A. (2003a). Thrombin and protease-activated receptor-1 agonists promote lipopolysaccharide-induced hepatocellular injury in perfused livers. *J. Pharmacol. Exp. Ther*. **305,** 417–425.

Copple, B. L., Ganey, P. E., and Roth, R. A. (2003b) Liver inflammation during monocrotaline hepatotoxicity. *Toxicology* **190,** 155–169.

Eguchi, Y., Shimizu, S., and Tsujimoto, T. (1997). Intracellular ATP levels determine cell death fate by apoptosis or necrosis. *Cancer Res*. **57,** 1835–1840.

Gordon, G. J., Coleman, W. B., and Grisham, J. W. (2000a). Bax-mediated apoptosis in the livers of rats after partial hepatectomy in the retrorsine model of hepatocellular injury. *Hepatology* **32,** 312–320.

Gordon, G. J., Coleman, W. B., Hixson, D. C., and Grisham, J. W. (2000b). Liver regeneration in rats with retrorsine-induced hepatocellular injury proceeds through a novel cellular response. *Am. J. Pathol*. **156,** 607–619.

Gujral, J. S., Knight, T. R., Farhood, A., Bajt, M. L., and Jaeschke, H. (2002). Mode of cell death after acetaminophen overdose in mice: apoptosis or oncotic necrosis? *Toxicol. Sci*. **67,** 322–328.

Huxtable, R. J. (1989). Human health implications of pyrrolizidine alkaloids and herbs containing them. In *Toxicants of Plant Origin*. (P. R. Cheeke, Ed.), Vol. 1, pp. 41–86. CRC Press, Boca Raton, FL.

Jaeschke, H., Farhood, A., Cai, S. X., Tseng, B. Y., and Bajt, M. L. (2000). Protection against TNF-induced liver parenchymal cell apoptosis during endotoxemia by a novel caspase inhibitor in mice. *Toxicol. Appl. Pharmacol*. **169,** 77–83.

Jaeschke, H., Fisher, M. A., Lawson, J. A., Simmons, C. A., Farhood, A., and Jones, D. A. (1998). Activation of caspase 3 (CPP32)-like proteases is essential for TNF-alpha-induced hepatic parenchymal cell apoptosis and neutrophil-mediated necrosis in a murine endotoxin shock model. *J. Immunol*. **160,** 3480–3486.

Kobayashi, H., Horikoshi, K., Yamataka, A., Yamataka, T., Okazaki, T., Lane, G. J., and Miyano, T. (1999). Hyaluronic acid: a specific prognostic indicator of hepatic damage in biliary atresia. *J. Pediatr. Surg*. **34,** 1791–1794.

Kubasiak, L. A., Hernandez, O. M., Bishopric, N. H., and Webster, K. A. (2002). Hypoxia and acidosis activate cardiac myocyte death through the Bcl-2 family protein BNIP3. *Proc. Natl. Acad. Sci. USA* **99,** 12825–12830.

Lafranconi, W., and Huxtable, R. (1984). Hepatic metabolism and pulmonary toxicity of monocrotaline using isolated perfused liver and lung. *Biochem. Pharmacol*. **33,** 2479–2484.

Lamy, L., Ticchioni, M., Rouquette-Jazdanian, A. K., Samson, M. Deckert, M. Greenberg, A. H., and Bernard, A. (2003) CD47 and the 19 kDa interacting protein-3 (BNIP3) in T cell apoptosis. *J. Biol. Chem*. **278,** 23915–23921.

Lawson, J. A., Fisher, M. A., Simmons, C. A., Farhood, A., and Jaeschke, H. (1998). Parenchymal cell apoptosis as a signal for sinusoidal sequestration and transendothelial migration of neutrophils in murine models of endotoxin and Fas-antibody-induced liver injury. *Hepatology* **28,** 761–767.

Lawson, J. A., Fisher, M. A., Simmons, C. A., Farhood, A., and Jaeschke, H. (1999). Inhibition of Fas receptor (CD95)-induced hepatic caspase activation and apoptosis by acetaminophen in mice. *Toxicol. Appl. Pharmacol*. **156,** 179–186.

Leist, M., Single, B., Castoldi, A. F., Kuhnle, S., and Nicotera, P. (1997) Intracellular adenosine triphosphate (ATP) concentration: a switch in the decision between apoptosis and necrosis. *J. Exp. Med*. **185,** 1481–1486.

Lemasters, J. J., Ji, S., and Thurman, R. G. (1981). Centrilobular injury following hypoxia in isolated, perfused rat liver. *Science* **213,** 661–663.

Mattocks, A. R., and White, I. N. H. (1970). Estimation of metabolites of pyrrolizidine alkaloids in animal tissues. *Anal. Biochem*. **38,** 529–535.

Nyska, A., Moomaw, C. R., Foley, J. F., Maronpot, R. R., Malarkey, D. E., Cummings, C. A., Peddada, S., Moyer, C. F., Allen, D. G., Travlos, G., *et al.* (2002). The hepatic endothelial carcinogen riddelliine induces endothelial apoptosis, mitosis, S phase, and p53 and hepatocytic vascular endothelial growth factor expression after short-term exposure. *Toxicol. Appl. Pharmacol*. **184,** 153–164.

Oinonen, T., and Lindros, K. O. (1998). Zonation of hepatic cytochrome P-450 expression and regulation. *Biochem. J*. **329,** 17–35.

Pan, L. C., Wilson, D. W., Lame, M. W., Jones, A. D., and Segall, H. J. (1993). Cor pulmonale is caused by monocrotaline and dehydromonocrotaline but not by glutathione or cysteine conjugates of dihydropyrrolizine. *Toxicol. Appl. Pharmacol*. **118,** 87–97.

Paxian, M., Bauer, I., Rensing, H., Jaeschke, H., Mautes, A. E. M., Kolb, S. A., Wolf, B., Stockhausen, A., Jeblick, S., and Bauer, M. (2003). Recovery of hepatocellular ATP and "pericentral apoptosis" after hemorrhage and resuscitation. *FASEB J*. **17,** 993–1002.

Raleigh, J. A., Chou, S. C., Tables, L., Suchindran, S., Varia, M. A., and Horsman, M. R. (1998). Relationship of hypoxia to metallothionein expression in murine tumors. *Int. J. Radiat. Oncol. Biol. Phys*. **42,** 727–730.

Regula, K. M., Ens, K., and Kirshenbaum, L. A. (2002). Inducible expression of BNIP3 provokes mitochondrial defects and hypoxia-mediated cell death of ventricular myocytes. *Circ. Res*. **91,** 226–231.

Schoental, R., and Head, M. (1955). Pathological changes in rats as a result of treatment with monocrotaline. *Brit. J. Cancer* **9,** 229–237.

Schultze, A. E., and Roth, R. A. (1998). Chronic pulmonary hypertension: The monocrotaline model and involvement of the hemostatic system. *J. Toxicol. Environ. Health B Crit. Rev*. **1,** 271–346.

Semenza, G. L. (1999). Regulation of mammalian O_2 homeostasis by hypoxia-inducible factor 1. *Annu. Rev. Cell Dev. Biol*. **15,** 551–578.

Sowter, H. M., Ratcliffe, P. J., Watson, P., Greenberg, A. H., and Harris, A. L. (2001). HIF-1-dependent regulation of hypoxic induction of the cell death factors BNIP3 and NIX in human tumors. *Cancer Res*. **61,** 6669–6673.

Steenkamp, V., Stewart, M. J., van der Merwe, S., Zuckerman, M., and

Crowther, N. J. (2001). The effect of *Senecio latifolius*, a plant used as a South African traditional medicine, on a human hepatoma cell line. *J. Ethnopharmacol*. **78,** 51–58.

Thomas, H. C., Lame, M. W., Dunston, S. K., Segall, H. J., and Wilson, D. W. (1998). Monocrotaline pyrrole induces apoptosis in pulmonary artery endothelial cells. *Toxicol. Appl. Pharmacol*. **151,** 236–244.

Thurman, R. G., Ji, S., Matsumura, T., and Lemasters, J. J. (1984). Is hypoxia involved in the mechanism of alcohol-induced liver injury? *Fundam. Appl. Toxicol*. **4,** 125–133.

Vande Velde, C., Cizeau, J., Dubik, D., Alimonti, J., Brown, T., Israels, S., Hakem, R., and Greenberg, A. H. (2000). BNIP3 and genetic control of necrosis-like cell death through the mitochondrial permeability transition pore. *Mol. Cell. Biol*. **20,** 5454–5468.

Yacoub, L. K., Fogt, F., Griniuviene, B., and Nanji, A. A. (1995). Apoptosis and bcl-2 protein expression in experimental alcoholic liver disease in the rat. *Alcohol Clin. Exp. Res*. ***19*,** 854–859.

Yee, S. B., Kinser, S., Hill, D. A., Barton, C. C., Hotchkiss, J. A., Harkema, J. R., Ganey, P. E., and Roth, R. A. (2000). Synergistic hepatotoxicity from coexposure to bacterial endotoxin and the pyrrolizidine alkaloid monocrotaline. *Toxicol. Appl. Pharmacol*. **166,** 173–185.